INVESTIGATIONS OF PERFORATED LAMINATES IN THE PRESENCE OF RESIDUAL STRESSES

D.H. Pahr,[1] C. Schuecker,[2] F. G. Rammerstorfer, [1]
H. E. Pettermann[1]

[1] Institute of Lightweight Design and Structural-Biomechanics, Vienna University of Technology, Gusshausstrasse 27-29, Vienna Austria
[2] Austrian Aeronautics Research / Network for Materials and Engineering (AAR)

ABSTRACT

Finite element based first ply failure strength investigations of perforated laminates in the presence of residual ply stresses are presented. Unit cell models are applied, where inter- and intra-laminar failure as well as free edge effects is taken into account on the ply level. The critical stress states contain constant and variable stress parts, which mean that non-radial loading paths are considered. Failure envelopes are computed for different lay-ups and residual stress levels. This way the strength evaluation of structures containing perforated laminates can be performed on the macroscopic, i.e. structural, level.

1. INTRODUCTION

Perforated layered laminates (see Figure 1) are applied in aerospace structures, e.g., as face sheets in sandwich compounds designed for absorbing noise, so called acoustic laminates.

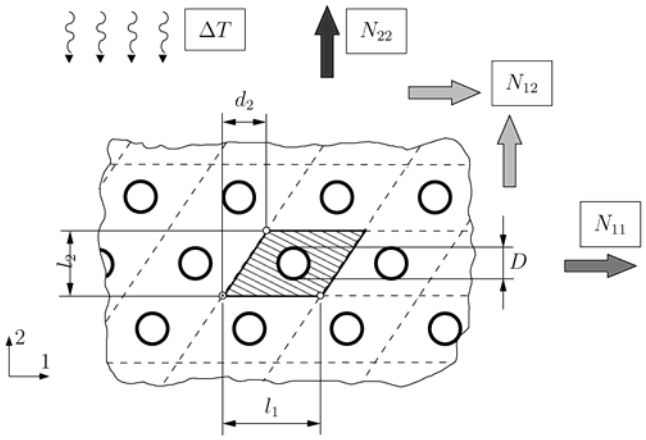

Fig. 1. Perforated laminate: Geometry, arrangement, and load cases of the unit cell, where $d_2 = 0$ corresponds to rectangular hole pattern

However, in most cases they must carry mechanical loads as well. Hence, the effective (macroscopic) stiffness behavior, the local stress distribution in the individual layers, and the effective strength of perforated laminates are of interest. The holes of the perforated laminate are drilled after curing. In previous works (see [1], [2]) the mechanical behavior of laminates loaded radially in stress space has been studied, where a fast multi-scale analyzing tool was introduced for the prediction of first ply failure (FPF) of structures containing perforated laminates. Experimental results were presented for the verification of numerical computations (see [2], [3]). A further step in the field of perforated laminates is the investigation of material behavior in the presence of residual ply stresses (self equilibrated on the laminate level).

Failure investigations with respect to this work can be structured as follows:

(1) Failure behavior of laminates,
(2) Failure behavior of laminates in the presence of residual stresses, and
(3) Failure behavior of laminates in the presence of residual stresses as well as high stress gradients (e.g., holes).

Starting with item (1), the first ply *failure behavior of laminates*, the assessment of risk of failure is mainly based on ply stresses computed from analytical models (CLT . . . Classical Lamination Theory [4]) and/or numerically. The obtained ply stresses can be used for comparing them with well known failure criteria: maximum stress, Tsai-Hill [4], Tsai-Wu [5], Puck criterion [6], etc. A comparison of a number of failure criteria can be found in [7], [8], [9]. Since in the most structural analyses residual stresses are not taken into account, the above failure models are based on radial load paths for the evaluation of a ply safety factor ${}^m\lambda$, i.e., ${}^m\sigma_{ij}\ {}^m\lambda = {}^m\sigma^*_{ij}$ with ${}^m\sigma_{ij}$ as the actual and ${}^m\sigma^*_{ij}$ as critical stress state of ply *m*.

For the first ply *failure behavior of laminates in the presence of residual stresses* (item (2)) the load paths are not radial anymore, and a constant (i.e. independent of external load) stress part appears. Residual stresses are usually defined as stresses which remain in mechanical parts, where they are not subjected to any external loading. The external loading can be mechanical, thermal, hygroscopic, etc. In order to define the situation "not subjected to external loading" a reference state has to be specified. The reference state is that state in which only the residual stresses exist and, for example, zero mechanical loading as well as a distinct temperature/moisture of the environment is evident. That means that residual stresses are in general related to a reference state. Residual stresses mainly come from (see [10], [11]):

- Manufacturing processes (e.g. pre-stressed roving, curing processes including chemical shrinkage, and thermal loading due to cool-down from curing temperature, etc.) and
- Environmental effects (hygro-thermal loading).

They are decreased by relaxation and aging processes. Residual stresses exist at different levels (length scales), generally divided into three, depending on the length scale on which the stress is observed:

- 1st level stresses, on the fiber/matrix level (micro-scale),
- 2nd level stresses, on the ply level (meso-scale), and
- 3rd level stresses, on the structural level (macro-scale).

They can be further categorized by their cause, e.g., thermal or elastic mismatch. This work is focused on the 2nd level residual stresses caused by thermal ply CTE mismatch. Residual stresses are special "constant stresses". In general constant stresses are stresses in mechanical parts which are subjected to any constant external loading (e.g., constant pressure, constant temperature/moisture difference with respect to the reference state).

Analytical methods which take "constant stresses" into account in failure assessment analyses can be found in [12], [13]. There, a superposition of constant (${}^m\sigma^c_{ij}$) and variable stresses (${}^m\sigma^v_{ij}$) of the form ${}^m\lambda\ {}^m\sigma^v_{ij} + {}^m\sigma^c_{ij} = {}^m\sigma^*_{ij}$ is assumed. Of course this assumption is only valid for linear elastic material behavior and a failure behavior that is independent of the loading path. Experimental investigations of Choo [14] verified that load path independency is only given for negligibly low material creep strains during loading. Experimental studies presented in [10] pointed out further problems: A poor correlation between experimental results and results from the theoretical stress analyses was found. There, it was suggested that further attention should be given to a robust cure model (evaluation of shrinkage strains) in order to obtain reliable residual stresses. A simple approach to obtain thermal residual stresses from curing is to choose an "effective stress free temperature" and compute the residual stresses with respect to a reference temperature (see Puck [6]). The effective temperature is smaller than, e.g., the curing temperature, which can be explained by relaxation processes.

A third important part (item (3)) in this study is the treatment of the first *ply failure behavior of laminates in the presence of residual stresses and holes* (perforated laminates). The challenge in dealing with this kind of laminates are the high stress concentrations (highly

inhomogeneous stress states) close to the free edge due to the geometrical stress concentration (notch effect of the holes) and due to the free edge effect. As mentioned before, a comprehensive study based on the mechanical behavior of such laminates can be found in [1], [2].

2. THEORETICAL BACKGROUND

2.1 Failure Models and Residual Stresses

Well known failure hypotheses, which are used in this work for the assessment of first ply failure, are:

- a combination of the maximum stress criterion [4] and 3D Tsai-Wu criterion [5] for fiber and inter-fiber failure,
- a quadratic criterion [16] for delamination, and
- the 3D Puck criterion [12], [6] is used additionally for all three failure modes.

In the case of the combined Tsai-Wu – maximum stress criterion the inner envelope of the failure surface is used, where only failure surfaces regarding normal stresses for the maximum stress criterion are considered (l, q, t direction). A common approach is that the variable stress state ${}^{m}\sigma_{ij}={}^{m}\sigma_{ij}^{v}$ and the FPF values (${}^{m}R_{ij}$) of a single ply *m* are used to compute a safety factor ${}^{m}\lambda$ for each individual layer/interface. The failure condition, $F = 1$, for each layer/interface can be written in a generalized form as

$$F({}^{m}\sigma_{ij}^{*},\ {}^{m}R_{ij}) = F({}^{m}\lambda\ {}^{m}\sigma_{ij}^{v},\ {}^{m}R_{ij}) = 1. \tag{1}$$

where ${}^{m}\sigma_{ij}^{*}$ is the critical stress state of ply/interface *m*. In the case of additional constant stresses, ${}^{m}\sigma_{ij}^{c}$, the actual stress state can be written in the form ${}^{m}\sigma_{ij}={}^{m}\sigma_{ij}^{v}+{}^{m}\sigma_{ij}^{c}$ and the failure condition, $F = 1$, for each layer/interface is extended to:

$$F({}^{m}\sigma_{ij}^{*},\ {}^{m}R_{ij}) = F({}^{m}\lambda\ {}^{m}\sigma_{ij}^{v} + {}^{m}\sigma_{ij}^{c},\ {}^{m}R_{ij}) = 1. \tag{2}$$

Figure 2 shows a graphic explanation of this definition of the safety factor. There, the constant, the variable, and the critical stress states are plotted for a schematic failure envelope.

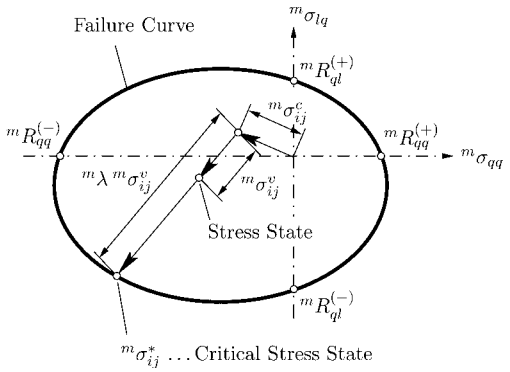

Fig. 2. σ_{qq}- σ_{lq} failure curve (failure envelope) including the definition of the safety factor ${}^{m}\lambda$ for ply *m*

For a laminate consisting of *n* layers and *n*-1 interfaces the safety factor of the laminate ${}^{lam}\lambda$ is given by

$${}^{lam}\lambda = \min_{n,n-1}({}^{m}\lambda, {}^{i}\lambda), \tag{4}$$

where the superscripts m and i denote the considered ply and interface, respectively. In the following this safety factor is used for plotting the macroscopic FPF envelopes.

2.2 Failure Models for Perforated Laminates and Characteristic Distance

Numerous failure models have been developed for strength prediction in notched laminates. Overviews are given in [17], [18]. These models can be classified into: First Ply Failure models (fracture mechanics models or stress based fracture models) and progressive failure models, respectively. The present work is focused on stress based FPF models going back to Withney and Nuismer [15]. There, it is assumed that failure of a notched laminate occurs when an average ply stress is equal to the FPF strength of an un-notched ply. The radial averaging distance is denoted as a_0 and is a key parameter for such models. Experimental and numerical investigations of this parameter (see [1], [2]) showed that the magnitude of a_0 is approximately one ply thickness and depends mainly on the material system (material and ply thickness) for first ply failure strengths predictions. For this work we choose the averaging distance a_0 as one ply thickness t_s, which is a conservative assumption.

The failure investigations described here are based on linear 3D finite element unit cell calculations (where inter-laminar stresses are taken into account, too), un-notched first ply failure strength values, and averaged stress values. The stress averaging for both, constant and variable stress parts is performed in radial direction with respect to the hole. Additional stress averaging through the layer thickness is not performed, which is conservative with respect to the used Puck criterion.

2.4 Unit Cell Analyses - Model

The local, i.e., unit cell analyses are demonstrated by examples with different lay-ups and residual stresses. In the following a global unit cell coordinate system denoted with 1, 2, 3 (see Figure 1) and a local ply coordinate system denoted with *l, q, t* are used (*l* is the fiber direction, *q* is the in-plane transverse direction, and *t* is the out-of-plane transverse direction). The ply angle is then defined as the angle between the local *l* and global 1-axis, where it is assumed that the 3 and *t* directions coincide.

2D and 3D finite element (FE) unit cell models are investigated. Algorithms are developed for implementing the homogenization methods, i.e. application of periodic boundary conditions and computation of macroscopic stiffness, i.e. on the laminate level, and strength values, as well as for the computing of the failure surfaces (for more details see [1], [2]). These algorithms take access to a standard displacement based FE-solver (ABAQUS) for the unit cell analyses. Linear Quad and Hex Elements are used. Typical unit cell model sizes are about 2000 elements for the 2D models and 7000 elements for the 3D models. In 3D models each ply is modeled with a minimum of four Hex Elements in thickness direction. Within the averaging length, a minimum of five elements is used. Mesh density studies are performed, and the error in the stiffness and strength values of the used meshes is found to be less than 2%. For the reliability of the finite element method for calculating free edge stresses in composite materials the guidelines of Whitcomb [19] are used as proven to be acceptable in [20].Figure 1 shows the geometry of a typical unit cell. The dimensions are D=1.5 mm, l_1=4.6 mm, l_2=3.98, d_2=2.3 (hexagonal arrangement of holes used in the considered example). The perforation area, i.e. the fraction of the area of the hole cross section, is about 10% of the total unit cell area.Figure 1 also shows the loading conditions. The unit cell is loaded with four different unit load cases, three mechanical and one thermal load case. The mechanical load cases are unit load cases of the membrane forces N_{11}, N_{22}, and N_{12}. The temperature load case consists of a uniform distributed temperature over the laminate.

These different load cases are linear superposed in order to obtain the presented results for radial load paths, as well as combined (thermo- mechanical) loading.

The used uni-directionally reinforced graphite/epoxy layers have a ply thickness of 0.2 mm. The major mechanical properties are E_l=125 GPa, E_q=8 GPa, E_t=8 GPa, G_{lq}=G_{lt}=5 GPa, G_{qt}=4 GPa, ν_{lq}= ν_{lt}=0.3, ν_{qt}=0.49, R_{l+}=1600 MPa, R_{l-}=1000 MPa, R_{lq+}=40 MPa, R_{q-}=220 MPa, R_{t+}=40 MPa, R_{t-}=220 MPa, R_{ql}=R_{lt}=80 MPa, R_{qt}=65 MPa, α_l=-0.45x10^{-6} 1/K, α_q= α_t=30x10^{-6} 1/K. At the interface the inter-laminar strength values ($R_{l+}^{IL}, R_{qt}^{IL}, R_{lt}^{IL}$) are based on the corresponding ply values (R_{t+}, R_{qt}, R_{lt}) reduced by a weakening factor of f_{wl}=0.8 (see [12]). All strength values are first ply failure strengths which can be obtained experimentally, e.g., by the acoustic emission testing technique (see [2]). The interaction parameter for the Tsai-Wu criterion is chosen to be 0.0 (see [4]). Parameters for the Puck criterion are on the one hand the gradients of the failure curves which are p_{qt+}=0.27, p_{qt-}=0.27, p_{ql+}=0.35, p_{ql-}=0.3 (taken from [21]) and on the other hand the empirical parameters for the influence of the longitudinal stress σ_{ll} on the inter-fiber failure, which are chosen as n=7 and $|\sigma_{ll}|$=1.1 $R_{l\pm}$ (for a detailed description see [12]). The investigated laminates are composed of three layers with a [0/α/0] lay-up, where α is variable.

3. RESULTS & DISCUSSION

Parametric studies are carried out. From the huge body of computational data only selected results are presented. They are chosen in order to be representative for other test cases which are not shown here.

3.1 Comparison of Various Failure Criteria (Non-perforated Laminates)

The goal of this section is twofold. On the one hand the differences between the two failure criteria (combined Tsai-Wu – maximum stress versus Puck criterion) should be pointed out. On the other hand the development of the critical failure surface should be discussed briefly. Figure 3 and Figure 4 show macroscopic single-layer FPF curves in the N_{11}- N_{22} membrane force space of a non-perforated [0/45/0] UD laminate for a 0° and the 45° layer.

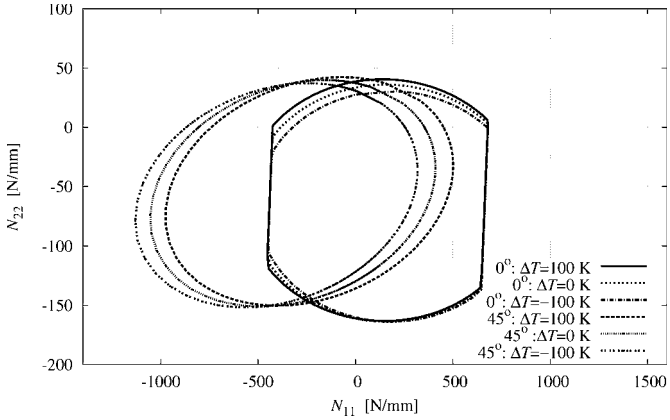

Fig. 3. Combined Tsai-Wu – maximum stress single-layer first ply failure curves of a non-perforated [0/45/0] UD laminate for a 0° and 45° layer based on residual stresses obtained from different temperature differences ΔT = 100, 0, -100 K.

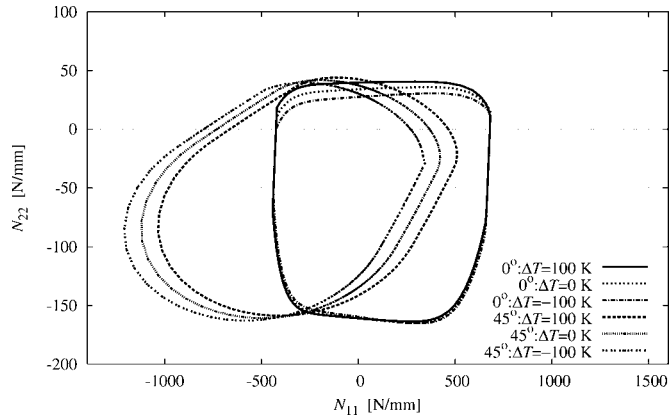

Fig. 4. Puck single-layer FPF curves of a non-perforated [0/45/0] UD laminate for a 0° and 45° layer based on residual stresses obtained from different temperature differences ΔT = 100, 0, -100 K.

N_{ij} denotes the stress resultants, i.e. the membrane force per unit width. They are based on residual stresses obtained from different temperature differences ΔT = 100, 0, -100 K, where the temperature difference ΔT is defined as reference temperature minus stress free temperature. A comparison of Figure 3 and Figure 4 shows that inter-fiber failure is influenced by the different residual stress states, which is visible for the failure curves of ply two (45° ply). There, a shift of the failure curves occurs, which corresponds to the magnitude of the residual stresses. Regarding fiber failure, which is dominant in the 1-direction of ply one and three (0° plies), practically no influence of the residual stresses is visible. Based on these macroscopic single-layer FPF curves a critical laminate FPF curve can be obtained by using Equation (4). Such critical failure curves are shown in Figure 5.

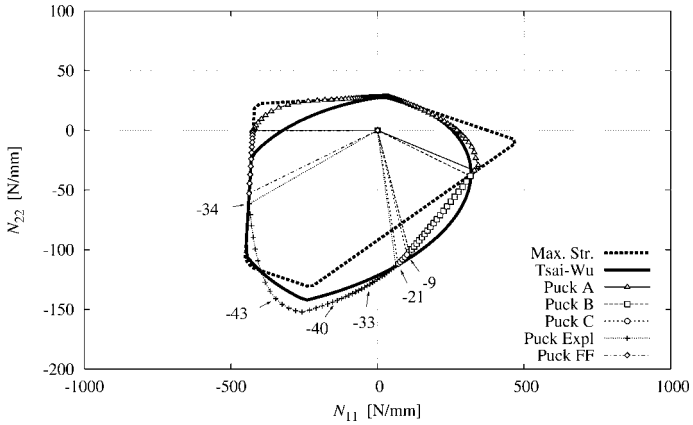

Fig. 5. Minimum laminate's first ply failure curve for the combined Tsai-Wu – maximum stress criterion, Puck criterion, and maximum stress criterion of a non-perforated [0/45/0] UD laminate based on residual stresses obtained from ΔT = -100. Numbers along the Puck curve belong to the inter-fiber fracture angle predicted by Puck's criterion

There, a maximum stress failure curve is also plotted in order to show the cut-off of the original Tsai-Wu failure curve. The combined Tsai-Wu – maximum stress and Puck's failure curve look very similar. In the case of the Puck criterion much more information is obtained for inter-fiber failure (see Puck curve in Figure 5). For example, the inter-fiber failure mode (Mode A, B, C), the risk of delamination (not active in this case) and explosion (wedge effect) of the laminate (see [6]) as well as the inter-fiber fracture angle (numbers along Puck curve in Figure 5). It should be mentioned that the Puck criterion is a phenomenological based criterion and is appropriate for uni-directional fiber reinforced laminates only.

3.2 Influence of Residual Stresses on FPF of Perforated Laminates, and Comparison of 2D/3D Results for a Selected [0/45/0] Lay-up

Figure 7 shows the influence of several residual stress states (ΔT = 200 … - 200 K) on the failure behavior of perforated and non-perforated [0/45/0] laminates based on Puck's criterion.

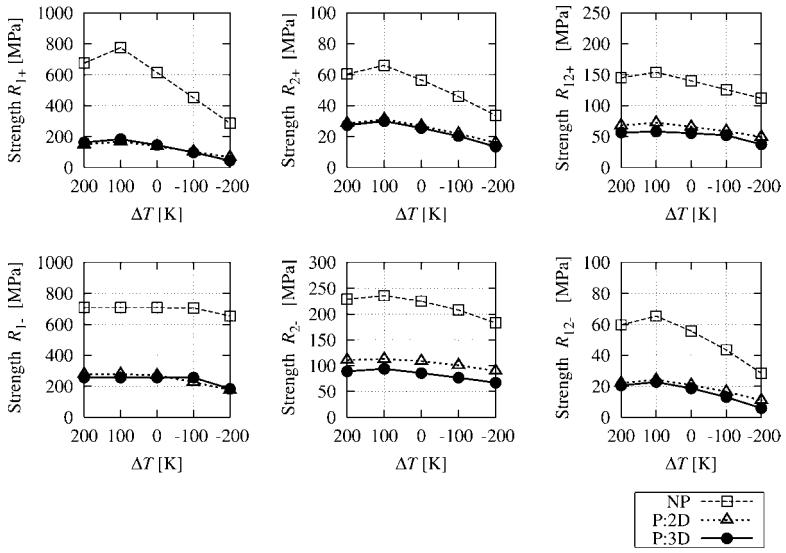

Fig. 7. Macroscopic FPF strengths ($= N_{ij\pm} \big/ t^{\text{lam}}$) of non-perforated (NP) and perforated (P) uni-directional [0/45/0] laminates with combined loading based on Puck's criterion

Each plot in Figure 7 corresponds to a tensile or compressive (denoted with "+" and "–", respectively) macroscopic in-plane strength" value, defined as $R_{1+} = \frac{N_{11+}}{t^{\text{lam}}}$, $R_{12+} = \frac{N_{12+}}{t^{\text{lam}}}$, etc ($t^{\text{lam}}$ . . . thickness of the laminate). A strong influence of both, the holes and residual stresses, on the macro-scopic perforated FPF strength is visible. For the stress free state (ΔT = 0 K) the macro-scopic perforated FPF strength values of the laminate decrease to approximately one third of the non-perforated values, although the perforated area is only 11.6%. A considerable influence of $\Delta T \neq 0$ is observed for the non-perforated and perforated strength values. Only the R_{1-} strength show practically no influence of residual stresses which can be explained by the fact the fiber failure is dominant for this load case (see also Figure 4). Regarding the shear FPF strength values R_{12+} and R_{12-} a noteable difference between both is evident, which comes from the [0/45/0] lay-up. Furthermore, the differences between results from 2D (open triangles) and 3D (solid circles) computations are presented in Figure 7. For most cases the differences are small and most of the 2D results predict too high strength values, i.e. they are not conservative. Therefore, 3D FPF results which also contain inter-laminar free edge stresses are to be used rather than 2D FPF results. Finally, it should be mentioned that the relative residual stress dependency is qualitatively the same for the non-perforated and perforated computations, i.e. they seem to be "scaled".

3.3 Influence of Residual Stresses on FPF of a [0/α/0] Lay-up with Variable Mid-layer Angle α

The influence of residual stresses on the macroscopic FPF strength values ($= N_{ij\pm} \big/ t^{\text{lam}}$) of non-perforated and perforated laminates, which are based on Puck's failure criterion, is shown for different [0/α/0] lay-ups in Figure 8.

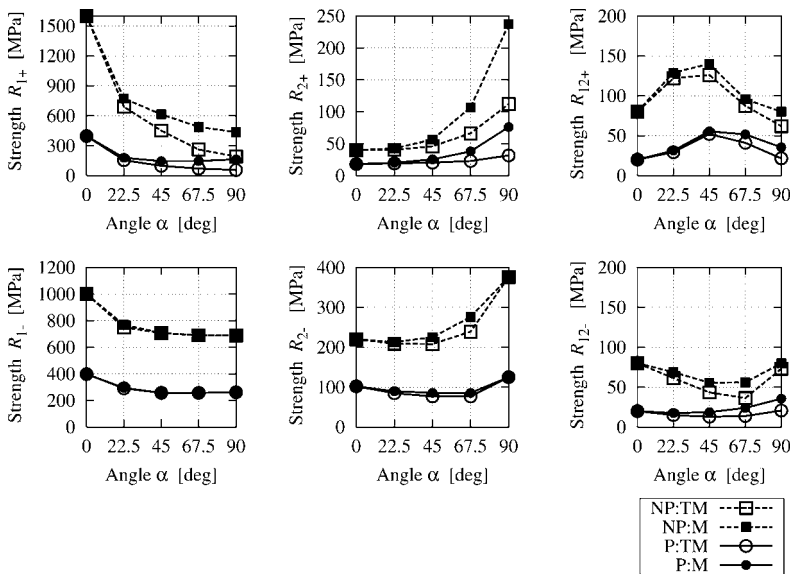

Fig. 8. Macroscopic FPF strengths ($= N_{ij\pm} \big/ t^{\text{lam}}$) of non-perforated (NP) and perforated (P, 3D based) uni-directional [0/α/0] laminates with mechanical (M) and combined loading (TM, ΔT = -100 K) for different mid-plane layer angles α based on Puck's criterion

There, four kinds of FPF strengths are compared: The macroscopic non-perforated FPF strength values of a laminate for mechanical (NP:M) and combined loading (NP:TM) as well as perforated macroscopic strength values for mechanical (P:M) and combined loading (P:TM), respectively. The temperature difference ΔT (reference temperature minus stress free temperature) is -100 K for all combined load cases. A strong impact of the residual stresses is visible for the R_{1+} and R_{2+} strength values for mid-layer ply angles greater then 45°. The largest difference between mechanical and combined load cases is observed for a [0/90/0] lay-up. In this case the thermal loading leads to the highest residual stresses. The other strength values show a small dependency on the residual stresses. A point which should be noticed is also the difference between the R_{12+} and R_{12-} curves. Even though the macroscopic shear strength values are equal for a [0/0/0] and [0/90/0] lay-up without residual stresses, huge differences between positive and negative shear strengths appear for the angles in between. The non-perforated and perforated FPF strength results look, except for a "scaling" of the curves, quite similar. In Figure 9 this fact is shown for a [0/45/0] lay-up and ΔT = -100 K.

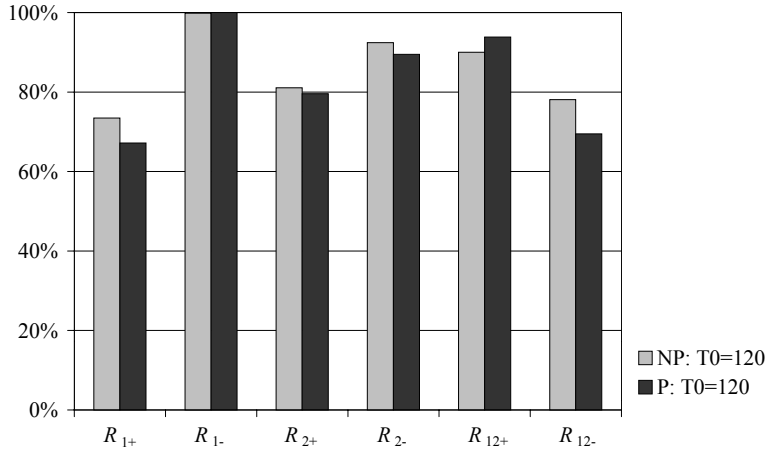

Fig. 9. Comparison of macro-scopic FPF strength reduction values of non-perforated (NP) and perforated (P)

There, the macroscopic FPF strength reduction values of non-perforated and perforated laminates are compared. Strength reduction refers to the difference between macroscopic non-perforated and perforated FPF strengths values with and without residual stresses, respectively. A good agreement between both degrees of reductions is observed, which means that for this kind of laminates and residual stresses, respectively, only the FPF strength behavior of the non-perforated laminate in the presence of residual stresses as well as the FPF strength behavior of the perforated laminate without any residual stresses is sufficient to make a rough prediction of the FPF strength behavior of the perforated laminate in the presence of residual stresses.

3.4 Delamination Sensitivity of a [0/45/0] laminate

The sensitivity of delamination of a [0/45/0] laminate is shown in Figure 10.

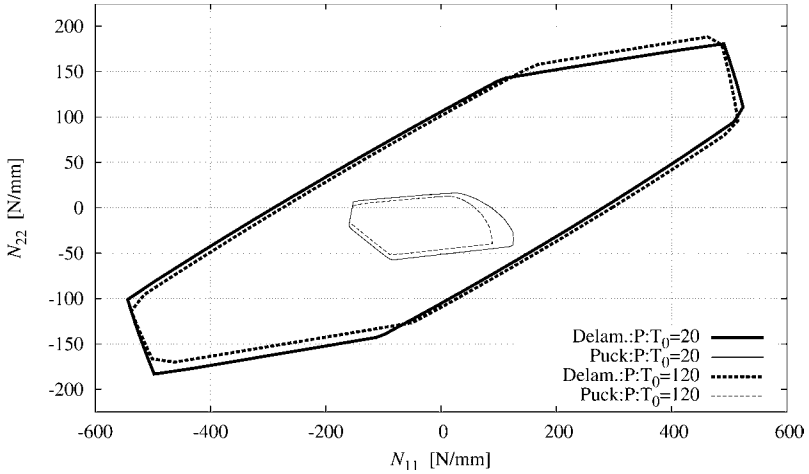

Fig. 10. Macro-scopic delamination and Puck's first ply failure curves of a perforated (P) [0/45/0] UD laminate for ΔT = 0 K (no residual stresses) and ΔT = -100 K

There, macroscopic delamination and Puck FPF curves of a perforated [0/45/0] UD laminate are plotted for ΔT = 0 K (no residual stresses) and ΔT = 100 K. Although an interface weakening factor of f_{wI}=0.8 is applied to the inter-laminar strength values, delamination is not critical for the cases with and without residual stresses. Previous investigations (see [2]) showed that interface weakening factors of approximately f_{wI}=0.3 would be necessary to obtain delamination failure in such laminates, which, of course, would indicate improper manufacturing of the laminate.

3. CONCLUSIONS

Various investigations with respect to the macroscopic first ply failure (FPF) behavior of non-perforated and perforated UD laminates in the presence of mesoscopic residual stresses are presented. A verification of the failure model shows that a combined Tsai-Wu – maximum stress criterion and the Puck criterion lead to similar failure predictions, where Puck's criterion gives additional information about the failure mechanism. A comparison of perforated 2D and 3D macroscopic FPF strength computations with and without residual stresses shows a rather small influence of the model (less than 25%). When non-perforated and perforated laminates are compared, the strongest FPF strength reduction arises from to the presence of the holes (reduction up to 22% of the non-perforated values, Figure 7). In both cases an influence of residual stresses on the FPF strength values is observed (maximum +28 … -57% of the residual stress free strength values), where the influence is less pronounced for perforated laminates. A dependency of the lay-up on the degree of reduction is found for [0/α/0] laminates if the mid-layer angle α is greater then 45°, which

can be explained by the increasing thermal expansion mismatch with an increasing mid-layer angle. Sensitivity studies regarding delamination failure point out that the investigated laminates are not sensitive to delamination, no matter whether residual stresses are present or not.

ACKNOWLEDGEMENTS

The financial support of the Austrian Federal Ministry of Economics and Labour within the Austrian Aeronautics Research / Network for Materials and Engineering (AAR) is gratefully acknowledged by CS and HEP.

References

1. **Pahr, D. H., Rammerstorfer, F. G.,** 2004. A fast multi-scale analyzing tool for the investigation of perforated laminates. *Comput. and Struct*. 82, 227-239.
2. **Pahr, D. H.,** 2003. Experimental and Numerical Investigations of Perforated FRP-Laminates. Fortschritt-Berichte VDI Reihe 18 Nr. 284. VDI Verlag, Düsseldorf, Germany.
3. **Pahr, D. H., Rammerstorfer**, F. G., 2003. Experimental and numerical investigations of perforated laminates. *Comp. Sci. and Tech*. in press.
4. **Jones, R. M**., 1999. Mechanics of Composite Materials. Taylor and Francis Inc., Philadelphia, USA, 2nd edn.
5. **Tsai, S. W., Wu,** E. M., 1971. A general theory of strength for anisotropic materials. *J. Comp. Mat*. 5, 58–80.
6. **Puck, A., Schürmann, H.,** 1998. Failure analysis of FRP laminates by means of physically based phenomenological models. *Comp. Sci. and Tech*. 58, 1045–1067.
7. **Soden, P. D., Hinton, M. J., Kaddour, A. S.,** 1998. A comparison of the predictive capabilities of current failure theories for composite laminates. *Comp. Sci. and Tech.* 58, 1225–1254.
8. **Soden, P. D., Hinton, M. J., Kaddour, A. S**., 1998. Lamina properties layup configurations and loading conditions for a range of fibre-reinforced composite laminates. *Comp. Sci. and Tech*. 58, 1011–1022.
9. **Hinton, M. J., Kaddour, A. S., Soden, P. D.,** 2002. A comparison of the predictive capabilities of current failure theories for composite laminates, judged against experimental evidence. *Comp. Sci. and Tech*. 62, 1725– 1797.
10. **Kaddour, A. S., Al-Hassani, S. T. S., Hinton, M. J.,** 2003. Residual stress assessment in thin angle ply tubes. *Appl. Comp. Mat*. 10, 169–188.
11. **Vasiliev, V. V., Morozov, E. V.,** 2001. Mechanics and Analysis of Composite Materials. Elsevier Science Ltd.
12. **Puck, A.,** 1996. Festigkeitsanalyse von Faser-Matrix-Laminaten. Carl Hanser Verlag München Wien, Germany.
13. **Palanterä, M., Klein, M.,** 1994. Constant and variable loads in failure analyses of composite laminates. *Computer Aided Design in Composite Material Technology* IV, 221–228.
14. **Choo, V. K. S.,** 1985. Effect of loading path on the failure of fibre reinforced composite tubes. *J. Comp. Mat.* 19, 525–532.
15. **Withney, J., Nuismer, R., 1974**. Stress fracture criterion for laminated composites containing stress concentrations. *J. Comp. Mat*. 8, 253–265.
16. **Brewer, J. C., Lagace, P. A.,** 1988. Quadratic stress criterion for initiation of delamination. *J. Comp. Mat*. 22, 1141–1155.
17. **Chu, G. G., Sun, C. T.,** 1993. Free edge and size effects on failure initiation and ultimate strength of laminates containing a center hole. In Proc. of 9th Int. Conf. on Composite Materials (ICCM/9 ’93), July 12–16, 1993, Madrid, Spain.
18. **Ng, S. P., Lau, K. J., Tse, P. C.,** 2000. 3D finite element analysis of tensile notched strength of 2/2 twill weave fabric composites with drilled circular holes. *Composites Part B* 31, 113–132.
19. **Whitcomb, J. D., Raju, I. S., Goree, J. G.,** 1982. Reliability of the finite element method for calculating free edge stresses in composite laminates. *Comput. and Struct*. 15, 23–37.
20. **Stiftinger, M., Rammerstorfer, F.,** 1996. Advances in Analysis and Design of Composites - Semi-Analytical Finite Element Formulations for Delamination Prediction in Layered Composite Structures, 61–72. Civil-Comp Press, Edinburgh.
21. **Puck, A., Kopp, J., Knops, M.,** 2002. Guidelines for the determination of the parameters in Puck’s action plane strength criterion. *Comp. Sci. and Tech*. 62, 371–378